ELSEVIER

Journal of Alloys and Compounds 271–273 (1998) 408–413

Journal of ALLOYS AND COMPOUNDS

Synchrotron radiation as a probe of actinide magnetism (T7-Al 'Magnetism')

D.B. McWhan*

Brookhaven National Laboratory, Bldg. 460, P.O. Box 5000, Upton, NY 11973-5000, USA

Abstract

Polarized beam experiments using synchrotron sources provide a direct measurement of both the orbital- and the spin-angular momentum densities. Similar information can be obtained by applying sum rules for the integral of the imaginary part of the forward-scattering amplitude over two spin-orbit split absorption edges to magnetic circular dichroism (MCD) measurements in ferri- and ferromagnetic materials. Large enhancements of the cross section for magnetic scattering at the M_{IV} and M_V absorption edges have led to studies of the weak critical scattering above magnetic phase transitions and of the order parameter in heavy fermion systems which have very small moments. These enhancements have also enabled studies of the modification of magnetic order in the near surface regions of crystals where the crystal symmetry is broken. © 1998 Elsevier Science B.V.

Keywords: X-ray scattering; Magnetic moments; Heavy fermion systems

1. Introduction

The realization that X-rays could be used to probe the magnetic properties of materials coincided with the development of synchrotron sources. In addition to their brightness, these sources combine the advantages of diffraction with those of spectroscopy in that they are tunable in energy and in polarization. As a result the use of synchrotron radiation in the study of magnetism has expanded rapidly [1]. Although neutron scattering has been the traditional probe of magnetism, X-ray scattering and absorption experiments are very complementary probes in the study of actinide compounds. First, is the inherent problem of available sample size where the brightness of synchrotron sources allows very intense beams to be focused onto very small samples. Second, is the discovery of very large enhancements in the magnetic scattering cross sections which occur at the M_{IV} and M_V absorption edges [2,3]. In this paper the cross-section for magnetic scattering and absorption experiments is summarized and examples of recent work on actinide compounds are reviewed. In principle, it is possible to measure directly both the orbital- (L) and the spin-(S) angular momentum densities using nonresonant magnetic X-ray scattering and by applying various sum rules to resonant scattering and absorption experiments. The ratio L/S is a well defined quantity in the 4f series but especially, in highly correlated systems such as heavy fermion superconductors, L/S is of current interest. Initial attempts to make these measurements on UAs [3,4] and US [5] are discussed in the second section. In the heavy fermion superconductors the magnetic moments are greatly reduced from the free-ion values and a full understanding of the interaction of the relatively localized 5f electrons with the metallic band states remains elusive. Recent resonant magnetic-scattering studies on these systems [6–8] are given in the third section. There is considerable interest in how the magnetic properties change on going from the bulk to the surface and in particular how the statistical mechanics of the phase transition are affected. The surface sensitivity of an X-ray experiment can be controlled by the geometry of the scattering experiment relative to the surface and studies of the surface of UAs [9] and UO_2 [10] are discussed in the fourth section.

2. Magnetic scattering and absorption

Following the initial suggestion by Platzman and Tzoar that X-rays could be used to determine magnetic structures [11], the seminal work by de Bergevin and Brunel gave a full theoretical development and experimental verification using a sealed tube X-ray source [12,13]. At high photon energies, which are far away from characteristic atomic

*Tel.: (516) 344-3927; fax: (516) 344-5584.

PII: S0925-8388(98)00100-5

energies, the weak direct interaction between the magnetic field of the photon and the fourier transforms of the orbital-, $\boldsymbol{L}(\boldsymbol{K})$, and spin-, $\boldsymbol{S}(\boldsymbol{K})$, angular momentum densities leads to a term in the atomic scattering factor of the form given by Blume [14] and Blume and Gibbs [15] of:

$$f(\boldsymbol{K})^{\mathrm{mag}} = ir_0 \frac{\hbar K}{mc}\left[\frac{1}{2}\boldsymbol{A}\cdot\boldsymbol{L}_{\mathrm{j}}(\boldsymbol{K}) + \boldsymbol{B}\cdot\boldsymbol{S}_{\mathrm{j}}(\boldsymbol{K})\right] \quad (1)$$

where r_0 is the electron radius, $\boldsymbol{K}=\boldsymbol{k}_{\mathrm{i}}-\boldsymbol{k}_{\mathrm{f}}$ is the momentum transfer, and $\boldsymbol{A}$ and $\boldsymbol{B}$ are complex matrices which depend on the wavevector and on the polarization of the incident and scattered photons. This magnetic scattering is much weaker than normal charge scattering, which varies as Zr_0, because of the factor $\hbar K/mc$, which is typically ~0.01. Because the contributions of the orbital and spin terms to the scattering amplitude depend differently on the polarization, it is possible to separate them experimentally if the scattering geometry is chosen appropriately and if the polarization of the incident and scattered photons is determined as demonstrated for the case of antiferromagnetic holmium metal [16]. The polarization dependencies of normal charge scattering and magnetic scattering are also different so that the two can be distinguished as demonstrated again in holmium [17].

At photon energies near to atomic absorption edges of magnetic ions in solids, there are both scattering and absorption (forward scattering) effects. The theory has been developed by Hannon et al. [18,19] for both dipole and quadrupole transitions, and extended by Luo et al. [20] in the fast-collision approximation for elastic and inelastic resonant X-ray scattering. The polarization dependence and correlation functions are given in Ref. [21]. Recently, Blume [22] pointed out that in deriving the orbital term in Eq. (1) a summation is made over all possible states and in order to avoid double counting in the resonant terms, a multiplicative term ω_0/ω where ω_0 is the resonant frequency of the dipole transition, has to be added to the equations given in Ref. [18,19]. The resulting atomic scattering amplitude for resonant magnetic X-ray scattering in the dipole approximation is given by:

$$f_{\mathrm{res}}^{\mathrm{mag}} = \frac{3\lambda\omega_0}{8\pi\omega}\{\boldsymbol{e}_{\mathrm{f}}^{*}\cdot\boldsymbol{e}_{\mathrm{i}}[F_{11}+F_{1-1}] - i(\boldsymbol{e}_{\mathrm{f}}^{*}\times\boldsymbol{e}_{\mathrm{i}}) \cdot\boldsymbol{z}_{\mathrm{J}}[F_{11}-F_{1-1}] + (\boldsymbol{e}_{\mathrm{f}}^{*}\cdot\boldsymbol{z}_{\mathrm{J}})(\boldsymbol{e}_{\mathrm{i}}\cdot\boldsymbol{z}_{\mathrm{J}})[2F_{10}-F_{11} - F_{1-1}]\} \quad (2)$$

where $\boldsymbol{e}_{\mathrm{j}}$ and $\boldsymbol{e}_{\mathrm{i}}$ are the polarization of the final and incident photons, and $\boldsymbol{z}_{\mathrm{J}}$ is the magnetization direction of the atomic magnetic moment. The terms F_{LM} where L is the order of the transition ($L=1$ for dipole transitions) and M is the change in angular momentum ($\Delta M=0, \pm1$), are composed of matrix elements which couple the ground and excited states via the dipole operator, the probabilities that the ground state is occupied and that the excited state is empty, and a resonant energy denominator. The first term is independent of the direction of the magnetic moment, and it leads to the usual anomalous-scattering corrections to the charge scattering. The second term is linear in the magnetic moment direction. The third term is quadratic in the moment direction. In an antiferromagnet, the second term produces reflections in reciprocal space at the wavevector of the magnetic structure and in a ferromagnet gives magnetic contributions to the charge reflections. For forward scattering the optical theorem relates the imaginary part of the forward scattering to the absorption coefficient:

$$\mu = 2\lambda NIm[f(\boldsymbol{k}_{\mathrm{f}}=\boldsymbol{k}_{\mathrm{i}},\boldsymbol{e}_{\mathrm{f}}=\boldsymbol{e}_{\mathrm{i}})] \quad (3)$$

In this case, the second and third terms lead to magnetic circular and linear dichroism, respectively [23]. MCD is the difference in the absorption coefficient for plus and minus helically polarized X-rays and linear magnetic dichroism is the difference for σ- and π-polarized X-rays. The second term is measured in a scattering experiment in both antiferromagnetic and ferromagnetic materials or in MCD experiments on ferromagnetic materials.

The resonant magnetic scattering from the antiferromagnet UAs is illustrated in Fig. 1 where the intensity of the (0, 0, 5/2) magnetic reflection is shown as a function of energy through the $\mathrm{M_V}$, $\mathrm{M_{IV}}$, and $\mathrm{M_{III}}$ edges. Note that this figure, unlike those in Refs. [1,2], includes the correction term derived by Blume [22] and this results in much better agreement in the tails of the resonances between the calculated curve, which is based on the sum of three coherent dipole oscillators, and the measurements reported in Ref. [2]. At the peak of the $\mathrm{M_{IV}}$ resonance, the intensity is approximately 1% of the intensity from a (002) charge reflection. This represents an enhancement of the magnetic scattering over the nonresonant terms in Eq. (1) of over six orders of magnitude. It is this enhancement that makes it possible to study materials with small magnetic moments and to study magnetic surface phase transitions.

Sum rules for the resonances observed at two spin orbit split absorption edges such as the L_{II} and L_{III} in transition and rare earth elements and the $\mathrm{M_{IV}}$ and $\mathrm{M_V}$ in actinide elements are given in terms of the absorption coefficient for circular polarization with positive and negative helicity by [24,25]:

$$\int_{j^+ + j^-} d\omega(\mu^+ - \mu^-) \Big/ \int_{j^+ + j^-} d\omega(\mu^+ + \mu^- + \mu^0) \simeq (1/2)C_{cln}\left\langle L_z(0)\right\rangle \quad (4)$$

$$\int_{j+1} d\omega(\mu^+ - \mu^-) - [(c+1)/c]\int_{j^-} d\omega(\mu^+ - \mu^-) \Big/ \int_{j^+ + j^-} d\omega(\mu^+ + \mu^- + \mu^0) \simeq D_{cln}\left\langle S_z(0)\right\rangle + E_{cln}\left\langle T_z\right\rangle \quad (5)$$

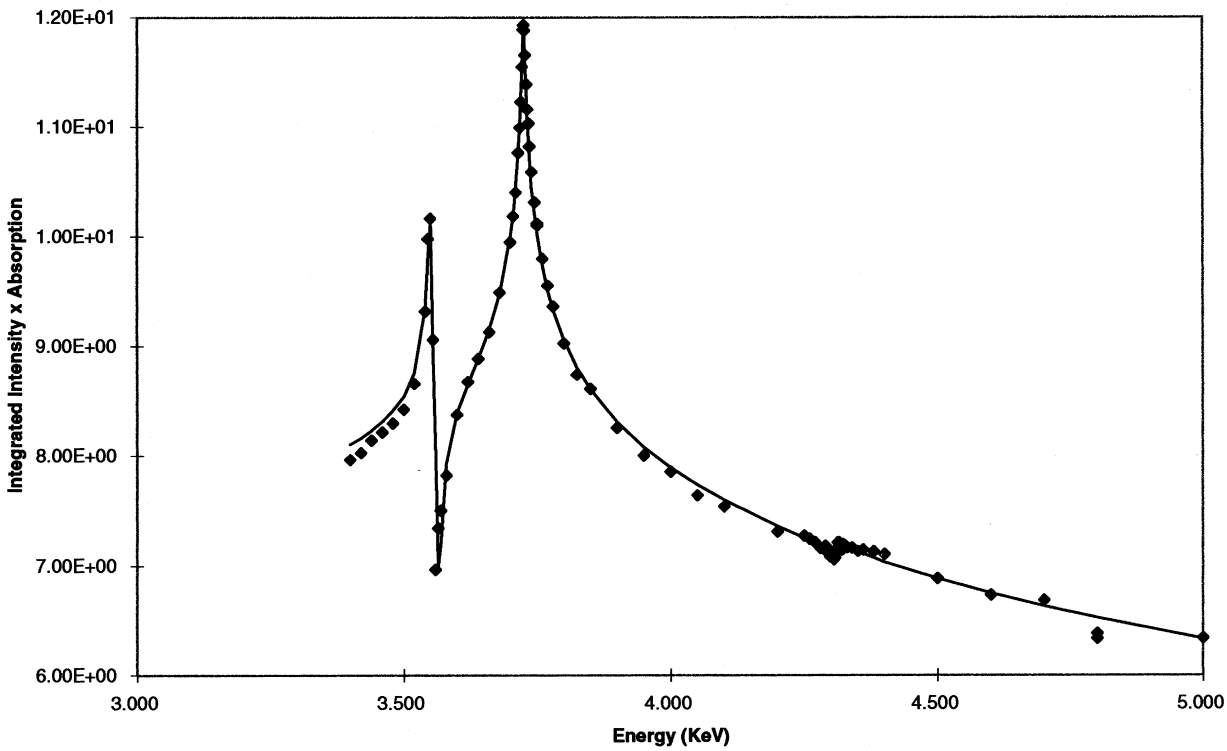

Fig. 1. Resonant magnetic scattering in uranium arsenide at the M_V, M_{IV} and M_{III} absorption edges of uranium. Solid curve through the data from [3] is the coherent sum of three quantum-mechanical dipole oscillators including the ω_0/ω term derived in [21].

where C_{cln}, D_{cln}, and E_{cln} are coefficients defined in terms of c and l which are the quantum numbers for the core and excited states, respectively, and n, which is the number of electrons in the ground state configuration. $L_z(0)$ and $S_z(0)$ are the ground-state expectation values for the orbital- and spin-angular momentum densities and T_z is a magnetic dipole term.

3. Separation of spin- and orbital-angular momentum densities in UAs and US

The resonant and nonresonant magnetic scattering described in Section 1 should provide new probes with which to gain insight into the wide variations in magnetic moment in actinide compounds. The application of these probes present both experimental and theoretical challenges. In nonresonant magnetic scattering, the intensity of a typical magnetic reflection in an antiferromagnet such as UAs will be approximately nine orders of magnitude smaller than the charge scattering. When coupled with the relative inefficiency of polarization analyzers, these measurements require intense synchrotron sources and judicious choices of scattering geometry to minimize the large background from the charge scattering. For resonant magnetic scattering and MCD experiments, it is the absorption problems associated with experiments at the energies of the M absorption edges (3–4 KeV) that have to be overcome. To date there have been two attempts to measure the orbital- and spin-angular momentum densities using nonresonant scattering techniques in UAs [2,4] and attempts using MCD in US [5], UFe_2 [26], and $USb_{0.5}Te_{0.5}$ [27].

The uranium monopnictides are a series of intermetallic compounds in which the 5f electrons become increasingly itinerant going up the series from UBi to USb to UAs to UN as evidenced by the decreasing magnetic moment from 3.0 to 0.7 Bohr magnetons. UA has the NaCl crystal structure and orders at $T_N = 127$ K in a type-I antiferromagnetic structure which changes at $T = 63$ K to a type-IA 2q structure which is accompanied by a discontinuous increase in the ordered moment from 1.9 to 2.2 μ_B/U [28]. The moment is substantially below the free-ion values expected for either $5f^2$ 3.28 μ_B or $5f^3$ 3.42 μ_B and it is of interest to have a direct measurement of the orbital- and spin-angular momentum densities.

Following Ref. [4] Eq. (1) can be expanded to give the magnetic matrix elements for the scattering processes for the α incident and β final polarization vectors as:

$$\left\langle M_{\mathrm{mag}}\right\rangle = \begin{bmatrix} \left\langle M_{\sigma\sigma}\right\rangle & \left\langle M_{\sigma\pi}\right\rangle \\ \left\langle M_{\pi\sigma}\right\rangle & \left\langle M_{\pi\pi}\right\rangle \end{bmatrix}$$

$$= \begin{bmatrix} S_1 \sin(2\theta) & 2\sin^2\theta[(\cos\theta)(L_2+S_2)+S_3\sin\theta] \\ -2\sin^2\theta[(\cos\theta)(L_2+S_2)-S_3\sin\theta] & \sin 2\theta[2L_1\sin^2\theta+S_1] \end{bmatrix} \quad (6)$$

where L_i and S_i refer to the Fourier components of the orbital- and spin-angular momentum densities, respectively. The subscripts 1, 2, 3 refer to the projections of the appropriate quantities along the axes U_i defined by the diffraction geometry of a given reflection (see Refs. [2,4]). σ is the polarization component perpendicular to the scattering plane, and π is the component within the scattering plane. Synchrotron radiation is linearly polarized in the plane of the electron orbit so that in a scattering experiment, the incident polarization can be either σ or π depending on whether the scattering plane is vertical or horizontal. In the experiments done on a bending magnet beamline (X16B) at the NSLS, a vertical scattering plane was used [2] and in the experiments done on the Troika (undulator) beamline at the ESRF, a horizontal scattering plane was used [4]. The choice of a horizontal scattering plane is a particularly judicious one because it minimizes the background resulting from charge scattering which varies as $e_i \cdot e_f$. In the vicinity of a scattering angle of 45°, the charge-scattering intensity is greatly reduced whereas both the $\pi\pi$ and the $\pi\sigma$ magnetic components are close to their maximum values.

In Ref. [2] the ratio of the $\sigma\pi$ component of the (0, $\pm 1/2$, 2) to the intensity of the (002) charge reflection was $1.0 \pm 0.5 \times 10^{-9}$ which is similar to the ratio calculated for the full free-ion value of 1.1×10^{-9}. Any extinction corrections to the observed intensity of the (002) would have the effect of lowering the observed ratio. In Ref. [4], five different magnetic reflections were measured and a comparison with the relative intensity of each reflection, calculated from the magnetic matrix elements as a function of μ_l/μ_s, gave a value of $\mu_l/\mu_s = -2.0 \pm 0.5$ (which corresponds to $L/S = -4 \pm 1$). This experimental value is closer to the ratio calculated for a $5f^3$ configuration of -2.58 than to the ratio for $5f^2$ of -3.30. In addition, a comparison was made between the calculated and observed ratios as a function of scattering vector, and reasonable agreement was observed with the calculated form factors.

MCD measurements on the ferromagnet uranium sulfide have been carried out on a bending magnet beamline at the Synchrotron Radiation Department at Daresbury. US has the NaCl crystal structure and orders at $T_C = 177$ K with an ordered moment of 1.7 μ_B/U. Synchrotron radiation from a bending magnet becomes increasingly circularly polarized when viewed from above or below the plane of the electron orbit. MCD measurements were made by extracting the photon beam at ± 0.10 mrad with respect to the electron orbit and measuring the absorption using fluorescence detection and reversing either the helicity of the photons by going above or below the plane or the magnetization of the sample with an electromagnet.

For US where the resonances involve transitions from 3d to 5f, $l = 3$, $c = 2$ and n is taken to be 2. The measured values for the various sums become [5]:

$$-0.100 = (1/3n_h)L_z \quad (7)$$

$$+0.121 = (2/3n_h)(S_z + 3T_z) \quad (8)$$

where $n_h = 4l + 2 - n = 12$ is the number of valence holes in the ground state. In order to find reasonable agreement between theory and experiment, it was necessary to go beyond the Hund's rule values and compute the $5f^2$ and $5f^3$ magnetic ground states including intermediate coupling and including a sizable calculated magnetic dipole term. This is in contrast to the transition metals where the dipole term is small. The experimental values are in between those calculated for the two configurations, and it is concluded that the ground state is a mixture of the two configurations with a crystal field. In order to compare the calculations with the values above, the authors had to scale the calculated values of L_z, S_z, and T_z to give the magnetic moment derived from neutron scattering experiments. The justification for scaling is that weak crystal fields will not effect the shape of the absorption spectra but only change the overall intensities and moments by a constant factor.

There is growing evidence that the branching ratio, which is the ratio of the intensity of the M_{IV} to that of the M_V, deviates substantially from the free-ion states of 17 ($5f^2$) and 6 ($5f^3$). For UO_2, a calculation including the full multiplet structure in intermediate coupling and a crystal field splitting established by neutron scattering gave a good fit to the measured resonant magnetic scattering data which has a branching ratio of 6–7 [29]. Other ratios which have been measured are: US 7.7 [5], UAs 11 [2], USb 3.5 [29]. These ratios are both larger and smaller than the value of 6 calculated for $5f^3$. It has been shown that the wide variation in branching ratio in the early actinides results largely from the changes in the magnetic dipole term with varying spin-orbit interaction [30]. Recently, it has been shown that the branching ratios at the rare earth L_{II} and L_{III} edges can be explained by a model in which the final state radial wave function contracts as a result of the 5d–4f spin–spin interaction thereby increasing the matrix element [31]. Thus, ratios are sensitive to spin-orbit coupling and final-state effects, and systematic measurements on series of actinide compounds will lead to a clearer understanding of these effects.

4. Heavy fermion superconductors

The low-temperature properties of heavy-fermion superconductors, which arise from the quantum-mechanical contact between the local f electrons and the metallic d band, continue to reveal a rich variety of magnetic and superconducting ground states. To date resonant magnetic scattering studies have been made on URu_2Si_2 [6], UPd_2Al_3 [7], and UPt_3 [8].

URu_2Si_2 orders antiferromagnetically at $T_N = 17$ K and then becomes superconducting at $T_C = 1.3$ K. UPd_2Al_3 orders at $T_N = 14.5$ K and becomes superconducting at $T_C = 2.0$ K. In both materials, no change is observed in

resonant magnetic scattering experiments in the magnetic order parameter on passing through the superconducting transition temperature [6,7]. However, a change in the magnetic phase is observed in UPd_2Al_3 at 11.8 K. The remarkable thing about these measurements is that they were done on a single microcrystallite at the surface of a polycrystalline boule.

In UPt_3 X-ray and neutron measurements show that the onset of superconductivity at 0.5 K changes the amplitude but not the direction of the ordered moments [8]. These authors also showed that the unusual splitting of the superconducting transition temperature, which occurs on annealing, has a similar effect on the magnetism in the near surface region probed by X-rays and in the bulk probed by neutrons. In all three materials, new information about these interesting heavy fermion materials has been obtained from resonant magnetic X-ray scattering measurements.

5. Surface effects

Over the last decade, surface X-ray scattering has been used to study the evolution with temperature of surface crystal structures which differs from the crystal structure of the bulk, and similar studies are now being performed on the changes in magnetic structures in the surface region. Measurements on UAs reveal that the surface layers order with a full magnetic moment of 3.5 μ_B [9]. The number of magnetically ordered layers increases and saturates at about 12 layers with decreasing temperature before the bulk first order transition occurs at which point the ordered moment of the surface layers decreases discontinuously to the bulk value.

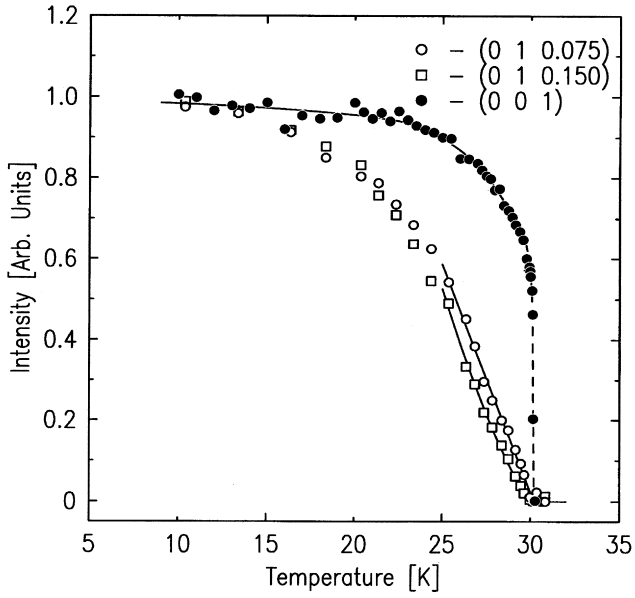

Fig. 2. Magnetic scattering from surface (open squares and circles) and bulk (solid circles) of uranium dioxide as a function of temperature showing surface-induced disorder [10].

In UO_2 a different evolution of surface magnetic scattering is observed. In Fig. 2, the intensity of the magnetic truncation rod as a function of temperature is compared with the specular Bragg reflection [10]. A first order transition occurs in the bulk, but the development of magnetic order in the surface region is continuous i.e., there is a surface induced disordering.

As a result of the resonant enhancement, it has been possible to study the magnetic critical scattering which develops above the Neél temperature in NpAs [32], UO_2 [33], UAs [34], UP [35], $USb_{0.8}$ $Te_{0.2}$ [36]. In a number of systems there are two length scales observed—a near-surface and a bulk length scale. The width of the surface phase is much larger than usually associated with surface effects and the origin of the near-surface effects are not well understood.

Acknowledgements

Useful discussions with M. Blume, D. Gibbs, G.H. Lander and C. Vettier are greatly appreciated. This work was supported by the U.S. DOE under contract No. DE-AC-02-CH7600016.

References

[1] D.B. McWhan, J. Synchrotron Rad. 1 (1994) 83–90.
[2] E.D. Isaacs, D.B. McWhan, C. Peters, G.E. Ice, D.P. Siddons, J.B. Hastings, C. Vettier, O. Vogt, Phys. Rev. Lett. 62 (1989) 1671–1674.
[3] D.B. McWhan, C. Vettier, E.D. Isaacs, G.E. Ice, D.P. Siddons, J.B. Hastings, C. Peters, O. Vogt, Phys. Rev. B42 (1990) 6007–6017.
[4] S. Langridge, G.H. Lander, N. Bernhoeft, A. Stunault, C. Vettier, G. Grubel, C. Sutter, F. de Bergevin, W.J. Nuttall, W.G. Stirling, K. Mattenberger, O. Vogt, Phys. Rev. B55 (1997) 6392–6398.
[5] S.P. Collins, D. Laundy, C.C. Tang, G. van der Laan, J. Phys. Condens. Matter 7 (1995) 9325–9341.
[6] E.D. Isaacs, D.B. McWhan, R.N. Kleiman, D.J. Bishop, G.E. Ice, P. Zschack, B.D. Gaulin, T.E. Mason, J.D. Garrett, W.J.L. Buyers, Phys. Rev. Lett. 65 (1990) 3185–3188.
[7] B.D. Gaulin, D. Gibbs, E.D. Isaacs, J.G. Lussier, J.N. Reimers, A. Schroder, L. Taillefer, P. Zschack, Phys. Rev. Lett. 73 (1994) 890–893.
[8] E.D. Isaacs, P. Zschack, C.L. Broholm, C. Burns, G. Aeppli, A.P. Ramirez, T.T.M. Palstra, R.W. Erwin, N. Stucheli, E. Bucher, Phys. Rev. Lett. 75 (1995) 1178–1181.
[9] N. Bernhoeft, A. Stunault, C. Vettier, F. de Bergevin, D. Gibbs, T.R. Thurston, S.M. Shapiro, J.B. Hastings, P. Dalmas, G. Helgesen, O. Vogt, J. Magnet. Magnetic Mat. 140–144 (1995) 1421–1422.
[10] G.M. Watson, D. Gibbs, G.H. Lander, B.D. Gaulin, L.E. Berman, Hj. Matzke, W. Ellis, Phys. Rev. Lett. 77 (1996) 751–754.
[11] P.M. Platzman, N. Tzoar, Phys. Rev. B2 (1970) 3556–3559.
[12] F. de Bergevin, M. Brunel, Acta Crystallogr. A37 (1981) 314–324.
[13] M. Brunel, F. de Bergevin, Acta Crystallogr. A37 (1981) 324.
[14] M. Blume, J. Appl. Phys. 57 (1985) 3615–3618.
[15] M. Blume, D. Gibbs, Phys. Rev. B37 (1988) 1779–1789.
[16] D. Gibbs, D.R. Harshman, E.D. Isaacs, D.B. McWhan, D. Mills, C. Vettier, Phys. Rev. Lett. 61 (1988) 1241–1244.

[17] D. Gibbs, D.E. Moncton, K.L. D Amico, J. Bohr, B. Grier, Phys. Rev. Lett. 55 (1985) 234–237.
[18] J.P. Hannon, G.T. Trammell, M. Blume, D. Gibbs, Phys. Rev. Lett. 61 (1988) 1245–1248.
[19] J.P. Hannon, G.T. Trammell, M. Blume, D. Gibbs, Phys. Rev. Lett. 62 (1989) 2644.
[20] J. Luo, G.T. Trammell, J.P. Hannon, Phys. Rev. Lett. 71 (1993) 287–290.
[21] J.P. Hill, D.F. McMorrow, Acta Cryst. A52 (1996) 236–244.
[22] M. Blume, in: G. Materlik, C.J. Sparks, K. Fischer (Eds.), Resonant Anomalous X-ray Scattering Theory and Applications, Elsevier Science, 1994, pp. 495.
[23] P. Carra, M. Altarelli, Phys. Rev. Lett. 64 (1990) 1286–1288.
[24] B.T. Thole, P. Carra, F. Sette, G. van der Laan, Phys. Rev. Lett. 68 (1992) 1243–1246.
[25] P. Carra, B.T. Thole, M. Altarelli, X. Wang, Phys. Rev. Lett. 70 (1993) 694–697.
[26] M. Finazzi, Ph. Sainctavit, A.-M. Dias, J.-P. Kappler, G. Krill, J.-P. Sanchez, P. Dalmas de Réotier, A. Yaouanc, A. Rogalev, J. Goulon, Phys. Rev. B55 (1997) 3010.
[27] P. Dalmas de Réotier, J.-P. Sanchez, A. Yaouanc, M. Finazzi, Ph. Sainctavit, G. Krill, J.-P. Kappler, J. Goedkoop, J. Goulon, C. Goulon-Ginet, A. Rogalev, O. Vogt, J. Phys. Condens. Matter 9 (1997) 3291.
[28] J. Rossat-Mignod, P. Burlet, H. Bartholin, R. Tchapoutian, O. Vogt, C. Vettier, R. Lagnier, Physica 102B (1980) 177.
[29] C.C. Tang, W.G. Stirling, G.H. Lander, D. Gibbs, W. Herzog, P. Carra, B.T. Thole, K. Mattenberger, O. Vogt, Phys. Rev. B46 (1992) 5287–5297.
[30] G. van der Laan, B.T. Thole, Phys. Rev. B53 (1996) 14458–14469.
[31] M. van Veenendaal, J.B. Goedkoop, B.T. Thole, Phys. Rev. Lett. 78 (1997) 1162–1165.
[32] S. Langridge, W.G. Stirling, G.H. Lander, J. Rebizant, Phys. Rev. B49 (1994) 12022–12029.
[33] G.M. Watson, B.D. Gaulin, D. Gibbs, T.R. Thurston, P.J. Simpson, S.M. Shapiro, G.H. Lander, Hj. Matzke, S. Wang, M. Dudley, Phys. Rev. B53 (1996) 686–698.
[34] S.C. Perry, W.J. Nuttall, W.G. Stirling, G.H. Lander, O. Vogt, Phys. Rev. B54 (1996) 10782–10790.
[35] A. Stunault, S. Langridge, C. Vettier, D. Gibbs, N. Bernhoeit, Phys. Rev. B55 (1997) 423–438.
[36] W.J. Nuttall, S. Langridge, W.G. Stirling, G.H. Lander, B. Lebech, O. Vogt, Phys Rev. B52 (1995) 4409.